Published in final edited form as:
Ann Biomed Eng. 2012 February ; 40(2): 408–421. doi:10.1007/s10439-011-0476-1.

The Role of Lymphatics in Cancer as Assessed by Near-Infrared Fluorescence Imaging

John C. Rasmussen[1], **Sunkuk Kwon**[1], **Eva M. Sevick-Muraca**[1], and **Janice N. Cormier**[2]

[1]Center for Molecular Imaging, The Brown Foundation Institute of Molecular Medicine, The University of Texas Health Science Center, Houston, 1825 Pressler St, SRB 330F, Houston, TX 77030, USA

[2]The University of Texas M.D. Anderson Cancer Center, Houston, TX, USA

Abstract

The lymphatic system is the secondary circulatory system responsible for fluid homeostasis and protein transport in the body. In addition, because the lymphatic system provides a primary pathway for cancer metastasis, lymph node involvement is routinely used as a determinant in cancer staging. Despite their importance, the lymphatics remain poorly understood, in part because of the historic lack of imaging modalities with sufficient spatial and/or temporal resolution to visualize the fine lymphatic structure and subtle contractile function. In recent years, near-infrared fluorescence (NIRF) imaging has emerged as a new imaging modality to non-invasively visualize the lymphatics and assess contractile lymphatic function in humans following administration of microdose amounts of a NIRF contrast agent. In this contribution, we first review NIRF imaging and its clinical application in sentinel lymph node mapping, intraoperative guidance, and assessing the architecture and contractile function of the lymphatics in health and in cancer-related lymphedema. We then present recent NIRF lymphatic imaging for non-invasive assessment of lymphatics both in preclinical melanoma models and in human subjects with melanoma.

Keywords

Imaging; Near-infrared fluorescence; Lymphatic; Metastasis; Lymphangiogenesis; Optics

INTRODUCTION

The importance of the hemovascular circulatory system has been long recognized to play a critical role in cancer progression.[11,15] Halting angiogenesis, or disrupting the process governing the formation and reorganization of the tumor neovasculature that provides nutrients for tumor expansion, is an emerging therapeutic strategy in cancer treatment.[9,19] However more recently, there has been increasing attention on the role of the lymphatic vasculature and disrupting the process of new lymphatic vessel formation (termed

Address correspondence to John C. Rasmussen, Center for Molecular Imaging, The Brown Foundation Institute of Molecular Medicine, The University of Texas Health Science Center, Houston, 1825 Pressler St, SRB 330F, Houston, TX 77030, USA. john.rasmussen@uth.tmc.edu.

ELECTRONIC SUPPLEMENTARY MATERIAL
The online version of this article (doi: 10.1007/s10439-011-0476-1) contains supplementary material, which is available to authorized users.

CONFLICT OF INTEREST
The authors report no financial conflicts of interest.

lymphangiogenesis) to arrest meta-static disease.[32,50] The emerging focus upon targeting lymphangiogenesis as a therapeutic strategy to arrest progressive cancer may not be surprising given the long standing clinical practice of lymph node (LN) dissection for (i) cancer staging based upon presence of cancer cells in resected LNs and (ii) regional control of disease associated with removal of potentially cancer-positive LNs and disruption of the lymphatic pathways involved in metastatic dissemination. Histological studies indicate that lymphangiogenesis may proceed prior to metastasis providing a cancer dissemination route.[45] For example, histological studies of resected human tissues have correlated an increased number or density of intra-and/or peri-tumoral lymphatic vessels with metastasis. [7,42] Dilation or increase in the cross-sectional area of intra-tumoral lymphatics has also been shown to be associated with metastatic melanoma. In addition, lymph sinus remodeling/dilation along with LN lymphangiogenesis in sentinel LNs (SLNs) and increased lymph flow to tumor-draining LNs have been shown to occur prior to LN metastasis in preclinical models.[16,40] Therefore, non-invasive imaging of changes in lymphatic function and remodeling may allow early identification of metastatic potential and lymphatic involvement. Yet the diagnostic tools to evaluate the *in vivo* status of tumor-induced lymphangiogenesis and to monitor the consequence of pharmacological interventions on the lymphatics remains lacking, due in part to the lack of imaging techniques than can accommodate the unique structure and function of the lymphatic circulatory system.

Compared to the hemovascular system, the lymphatic system is a poorly understood, unidirectional circulatory system comprised of initial lymphatic capillaries that take up fluid, macromolecules, cellular debris, and foreign contaminants from interstitial spaces. From the capillary plexus, lymph fluid is conducted *via* lymphatic vessels and trunks, through LNs for immune presentation and ultimately returns lymph fluid to the blood at the subclavian vein. In contrast to the hemovascular system, the lymphatics have no central pumping organ but instead, the lymphatic vessels are comprised of subunits called lymphangions that are bounded by valves and lined by smooth muscle cells. Lymph is actively “pumped” or propelled through the lymphangions *via* orchestrated peristaltic contractions and sequential closing/opening of valves. Additionally, hydrodynamic pressure gradients generated in surrounding tissues by extrinsic factors, such as skeletal muscle contractions, produce passive lymph flow without active lymphatic pumping. Given its diversity of function, the lymphatics have been implicated in a spectrum of diseases including cancer metastasis[41,50] and lymphedema, a disease which afflicts many cancer survivors in the U.S. (for review see Cormier *et al*.[6]).

Because lymph is typically translucent with relatively low concentrations of cells and particulate matter, there is little endogenous contrast available for conventional imaging of lymphatic vessels using X-ray, magnetic resonance imaging (MRI), and ultrasound techniques. Diagnostic lymphoscintigraphy is the only accepted method to image lymphatic function using 99mc-Technetium radiocolloid as a radiotracer administered subcutaneously in 1–5 cc volumes or intradermally in ~0.1 cc volumes. Intradermal administration results in efficient uptake of the radiocolloid by initial lymphatic capillaries and transport through lymphatic vessels to draining LNs. Upon decay, radiocolloid emits high energy gamma photons that efficiently propagate through tissues and are collected by a gamma camera for planar gamma scintigraphy. Planar gamma scintigraphy is performed over several minutes to identify tumor draining SLNs, visualize major lymphatic vessels, and diagnose lymphatic obstruction resulting in lymphedema.[59] Dynamic lymphoscintigraphy captures the advancing radiocolloid front transiting the lymphatics using a series of gamma images, acquired with exposure times as short as 20 s, to discriminate SLNs from those LNs that are secondary or drain the SLN.[25] However, lymphoscintigraphy suffers from several significant drawbacks for assessing tumor lymphangiogenesis including: (i) limited photon

count rate and sensitivity, (ii) finite radiocolloid size and comparatively long integration times that prevent direct imaging of contractile lymphatic function or active lymphatic pumping, and (iii) poor spatial resolution preventing visualization of small lymphatic neovasculatures that could characterize tumor lymphangiogenesis.

Opportunities for direct lymphangiography, similar to X-ray and magnetic resonance angiography, are limited due to the difficulties of cannulating lymphatic vessels and the transport of large volumes of viscous contrast agents.[4] Recent advancements in MRI contrast agents and faster imaging systems have enabled Liu *et al*.[26] to image anatomic and functional characteristics of diseased lymphatics using indirect lymphangiography in which contrast agent is injected intradermally, typically in the webs of digits. In their studies, interdigit injections of approximately 3 mL of gadobenate dimeglumine (GD) enabled MRI imaging of lymphatic vasculature and measurement of the transit speed of contrast moving from site of injection towards the draining LN basins in the legs of subjects with lymphedema. Yet the MRI approach failed to image lymphatic structure or movement of GD in healthy lymphatics owing, most likely, to significantly faster transit rates in the healthy as opposed to diseased lymphatics and the consequential lack of accumulated contrast agent required for MRI.

Over the past several years near-infrared fluorescence (NIRF) imaging has emerged as a non-invasive modality for *in vivo* lymphatic imaging in both animals[22,23,35,48,55] and humans.[34,43,44,47,57,58] NIRF imaging has been used intraoperatively to map the SLN and guide its surgical resection in cancer patients,[12,21,36,52] assess lymphatic structure and contractile function in health and disease,[34,43,44,47,57,58] and evaluate response to lymphedema therapy.[3,30,54] Herein we review the physics and instrumentation of NIRF imaging, briefly review its clinical application in the literature, and present our latest, NIRF images of longitudinal changes of the lymphatics in a preclinical model of progressing melanoma and snap shots in time of the lymphatics in melanoma patients.

PRINCIPLES AND INSTRUMENTATION OF NIRF IMAGING

NIRF imaging depends upon collecting the emitted photons following the activation of near-infrared (NIR) excitable fluorophores by absorption of tissue penetrating excitation light and subsequent radiative relaxation. The mean length of time between activation and radiative relaxation is called the lifetime and is typically on the order of nanoseconds. The number of fluorescent photons emitted over the excitation photons absorbed is defined as the quantum efficiency. Unlike a radioisotope that emits at most one photon event for nuclear imaging, a single fluorescent dye molecule can be excited multiple times and can theoretically emit hundreds of thousands of photons per second.[18] NIR light between the wavelengths of 780–900 nm is minimally absorbed by endogenous chromophores but is maximally scattered allowing it to propagate several centimeters into tissue. In addition, incident NIR excitation light produces little or no endogenous fluorescent signal, or autofluorescence, resulting in low background.[2] Yet unlike the high energy photons released from radioisotopes, NIR photons are of low energy and therefore highly scattered in tissues. As a result, despite the theoretically high photon count rates, tissue attenuation can limit the resolution of deep (>3–4 cm) fluorescently labeled tissues when planar NIRF approaches are used. As contained in several recent reviews, most human studies of NIRF imaging have focused upon intraoperative imaging, wherein tissue surfaces are imaged, or non-invasive imaging of superficial lymphatics, where the effects of scattering from superficial tissues are minimal.[29,38,46] NIRF tomography involves accounting for tissue scattering and absorption properties, and is under development for small animal imaging (see Stuker et al.[51] for review) and limited human studies.[5,33]

Contrast Agents

To date, all NIRF imaging studies in humans have employed indocyanine green (ICG) as the NIRF contrast agent.[29,38,46] ICG is a dark green, tricarbocyanine dye approved for intravenous use in humans for hepatic, cardiovascular, and ophthalmology applications. Although approved on the basis of its dark green color, in aqueous solution ICG has an absorption peak at 780 nm and is weakly fluorescent at a peak wave-length of at 800 nm. The quantum efficiency of ICG at excitation/emission wavelengths of 780/830 nm is 0.016,[13] reflective of its poor fluorescent properties. Nonetheless, due to the low autofluorescence of tissues the fluorescent signal emanating from ICG can be collected from deep in tissues. ICG lacks a functional group to which a targeting moiety, such as a peptide or antibody, can be attached for molecularly targeted imaging studies. Brighter NIRF contrast agents with functional groups to which molecular targeting moieties can be conjugated are in various stages of development and use in pre-clinical studies, however only IRDye 800CW has undergone safety and toxicity studies in preparation for human studies.[28] For lymphatic imaging, fluorescently labeled albumin protein and albumin binding domain peptides have been developed as NIRF contrast agents, but none are yet approved for use in humans.[8,27]

Instrumentation

Using microdose administration of ICG and NIR sensitive, intensified, charge coupled device (ICCD) cameras, our laboratories pioneered quantitative NIRF imaging of contractile lymphatic function in both animal and human subjects.[22,44,47,48] Figure 1a illustrates the custom-built fluorescent imaging systems used in our clinical imaging studies following the administration of ICG. The excitation source consists of a 500 mW 785 nm laser diode, collimating optics, and an engineered optical diffuser to illuminate a maximal tissue surface area of approximately 900 cm^2 with <1.9 mW/cm^2. 785 nm notch and 830 nm bandpass filters reject the backscattered excitation light and pass the emitted fluorescent signal from the surface tissues, respectively, through 28 mm Nikkor lens onto the photocathode of a Gen III image intensifier. The intensifier consists of three main components including the photocathode which converts the incident photons to electrons, the microchannel plate which uses a high voltage gain to multiply the electrons, and a phosphor screen which converts the multiplied electrons to photons. The intensified image on the phosphor screen is then acquired using a customized, 16-bit, frame transfer, charge coupled device (CCD) camera and saved to a computer. The CCD exposure time is typically 200 ms permitting near real-time imaging of the lymphatics *in vivo* and enabling the compilation of images into movies of lymph flow. The working distance of the system ranges from ~8 to ~30 inches as determined by the desired field of view. The imaging system is controlled using custom software developed in LabVIEW. For NIRF tomography, a signal generator and amplifiers can be used to modulate the laser diode intensity and intensifier photocathode voltage to obtain photon 'time-of-flight' information using the frequency-domain photon migration homodyne method.[20,56] As shown in Fig. 1b, the laser diode and camera are mounted on an articulating arm to facilitate camera manipulation for image acquisition in the clinic as well as operating suite.

As reviewed in Marshall *et al*.[29] clinical devices used thus far employ both intensified and non-intensified CCD systems. While the signal to noise ratio of ICCD systems is greater than that of non-intensified systems, [63] the image resolution is reduced owing to the configuration of the microchannel plate. Hence for smaller fields of view, as in the case of small animal imaging wherein resolution is important and higher doses of imaging agent may be tolerated, non-intensified CCD's may be more appropriate to employ than a more sensitive ICCD system. Therefore, for small animal imaging, planar fluorescent images are captured by an electron-multiplying CCD camera (EMCCD) and the associated optics used

in clinic with less than 200 ms integration time for dynamic imaging. In addition, a macrolens is also used to zoom in on a specific area of fluorescent lymphatic vessels.

Regardless of camera system, NIRF imaging can provide more rapid imaging of lymphatic function owing to the increased sensitivity associated with high photon count. However, the sensitivity of the NIRF imaging instrument is limited by the efficiency of rejecting excitation light while passing the fluorescent signal to the intensified photocathode or CCD. In a recent study the excitation light rejection efficiencies of different filter sets and filter positions were investigated, illustrating the importance of properly designed and positioned optics to reduce the imaging noise floor and thereby improve the system sensitivity and reduce the concentration of contrast agent required for visualization. [62] The current imaging configuration permits the use of microdose amounts of ICG which, as defined by the FDA,[14] is less than 1/100th of the pharmacological dose, less than 100 μg, or in the case of a protein based agent, less than 30 nmol. It is noteworthy that the ability to image humans following microdosage of a dim fluorescent dye such as ICG, suggests that brighter and molecularly targeted NIRF conjugates could in the future provide sensitive and disease specific information.

Image Analysis

Owing to the high photon count rate and low image acquisition times, NIRF imaging can be used not only to assess lymphatic structure but also to determine the apparent velocity of lymph propulsion and the period between consecutive lymphatic contractile events due to alternate contraction and relaxation of smooth muscle. As described in more detail in Rasmussen *et al*.[43] and illustrated in Fig. 2, quantification of the contractile lymphatic function, can be computed from the fluorescent profile along a lymphatic vessel as a function to time. Consider two regions of interest (ROIs) along the length of the lymphatic vessel and their average fluorescent intensity plotted as a function of time. The resulting profiles of fluorescent intensity as a function of time reflect the passage of packets of ICG-laden lymph through the region of interest. The apparent velocity can be calculated from the ratio of the apparent distance between the ROIs and the time required for the packet of lymph to propagate from one ROI to the other. The period between propulsions is the time lapse between the passage of two consecutive packets of ICG-laden lymph through the same ROI. The vessel tortuosity ratio is quantified by dividing the actual length of the lymphatic vessel by the distance between its ends.

REVIEW OF NON-INVASIVE NIRF LYMPHATIC IMAGING

Human Lymphatic Imaging

NIRF imaging has been used clinically to map the SLN and guide its surgical resection, to assess lymphatic structure and quantify its contractile function in health and disease, and to assess lymphatic response to therapy. A brief overview of each of these applications is provided below, for more extensive literature reviews (see Refs. [29,38,44,46]).

Perhaps the most widely reported clinical use of NIRF imaging has been SLN mapping and intraoperative imaging. In 2005, Kitai *et al*.[21] reported a 94% intraoperative detection rate of the SLN in a mapping study of 18 breast cancer patients following subcutaneous administration of 25 mg of ICG. This was followed by similar studies in gastric cancer[31] and skin cancer[12] also using milligram amounts of ICG. In 2008 Sevick-Muraca *et al*.[47] reported the use of NIRF imaging for SLN mapping using microgram amounts of ICG. In this dose escalation study, they reported propulsive lymph flow from injection sites on the breast to the SLN after administration of 10–100 μg of ICG. Ogata *et al*.[36] reported the use of NIRF imaging to intraoperatively guide lymphaticovenular anastamoses as surgical treatment for lymphedema.

In 2007, Unno *et al*.[57] reported the use of NIRF imaging to look at the lymphatics in the legs of 12 lymphedema and 10 control subjects following administration of 1 mg of ICG. In 2009 Rasmussen *et al*.[44] reported the use of NIRF imaging of the lymphatics in the arms or legs of 24 control and 20 unilateral lymphedema subjects following intradermal administration of ≤400 μg ICG. Distinct architectural differences between healthy lymphatics and diseased lymphatics (Fig. 3) were observed in both studies though only Rasmussen *et al*. reported propulsive lymphatic function as shown in online Video 1. While the lymphatics in control subjects tend to be straight and well defined (Figs. 3a and 3b), the lymphatics of subjects with lymphedema typically present with one or more of the following lymphatic abnormalities: dense networks of fluorescent lymphatic capillaries, tortuous vessels, and diffuse extravascular fluorescence (Figs. 2c and 2d). In 2010, Rasmussen *et al*.[43] reported the quantitative results of the imaging study and noted that while similar average propulsion velocities were observed in healthy limbs and in limbs with lymphedema, a significant reduction in the overall propulsion rate in the diseased limbs was observed, indicative of reduced lymphatic function in the diseased limbs.

In 2010 a technology assessment report commissioned by the United States Department of Health and Human Services decried the lack of evidence for an optimal test or treatment for lymphedema or an optimal means to assess the effectiveness of lymphatic treatments.[37] Recent publications indicate that NIRF imaging may provide a means to assess the effectiveness of lymphatic treatments by directly measuring lymphatic “pumping” or contractile function. Tan *et al*.[54] reported an improvement in contractile lymphatic function following MLD in both control limbs and limbs with lymphedema. Adams *et al*.[3] reported the use of NIRF imaging to assess the effectiveness of a pneumatic compression device designed to stimulate lymphatic flow from the affected arm towards the axilla in subjects with breast cancer-related lymphedema. In yet another study, Maus *et al*.[30] reported on the use of NIRF imaging to direct MLD in a subject with head and neck lymphedema following multiple surgeries to remove oral cancer.

Small Animal Lymphatic Imaging

NIRF imaging of the lymphatics in small animals has been also widely employed to map lymphatic drainage and SLN following injection of ICG, quantum dots, or NIR fluorophore conjugated molecules, such as antibody and proteins (for review see Zhang *et al*.[60]). While contractile lymphatic function was first observed in guinea pigs and rats in 1927[10] and mice in 1949[49] following surgical dissection, it was only recently that we non-invasively demonstrated, murine lymph propulsion in the limb, the tail, and the whole body of healthy immunodeficient nude and immunocompetent C57BL6 mice following intradermal injection of 2–10 μL of ICG.[22,24] Subsequently, we showed abnormal lymphatic drainage and function in tumor-bearing mice[23] and mice with lymphatic disorders.[24] Furthermore, altered contractile lymphatic function was observed in mice and rats fed a high salt diet (unpublished data). In addition to these studies, Zhou *et al*.[61] also reported changes of lymphatic drainage patterns and contractile function in mouse models of arthritis.

Below, we describe recent studies in which lymphatics were imaged both in a preclinical model of melanoma and in human melanoma patients using NIRF planar imaging.

NIRF IMAGING OF LYPMHATICS IN MELANOMA

Animal Studies

Experiments were performed in accordance with the guidelines of the Institutional Animal Care and Use Committee and approved by University of Texas Health Science Center at Houston Institutional Animal Care and Usage Committee in accordance with National Institutes of Health guidelines. All animals used in this study were maintained in a

pathogen-free mouse facility accredited by the American Association for Laboratory Animal Care.

Following cultivation, B16F10 cells, a murine melanoma cell line, were transfected with p-DsRedExpress- N1 (Clontech, CA) to generate DsRed expressing B16F10 cells (DsRed-B16F10). B16F10 or DsRed-B16F10 cells (10^6 cells per mouse) were then implanted intradermally in the dorsal aspect of the foot in 4–6 week old C56BL6 mice (Charles River, Wilmington, MA). Tumor-bearing mice were imaged up to 28 days post implantation (p.i.). Prior to imaging, 2 μL of a solution of 645 μM ICG in saline was injected intradermally at the web of the skin between the second and third digits of each hind foot using a 10 μL Hamilton syringe. Fluorescence images were acquired immediately before and for up to 30 min after injection.

Figure 4 represents NIRF images, from one representative mouse bearing B16F10 melanoma cells in the dorsal aspect of left hind foot (white arrow), showing progressive changes of lymphatic drainage during tumor growth. In addition, leaky, tortuous, and mispatterned lymphatic vessels were visualized. However, the patterns of lymphatic drainage in the contralateral right foot did not change. CT images at day 28 indicated that the tumor-draining LNs were progressively swollen, presumably due to metastatic disease, though future studies are needed to determine if the lymphatic reorganization/remodeling was due to tumor signaling, embolism, or another phenomenon.

Primary melanoma tumors often develop in-transit metastasis in the direction of lymph flow. As shown in Fig. 5, we found that a DsRed-B16F10 melanoma tumor in the dorsal aspect of foot formed in-transit metastases in lymphatic vessels. In addition, tortuous lymphatic vessels and dye leakage proximal to the primary tumor were observed around the in-transit metastases. The ability to see in-transit metastases indicates that NIRF imaging, with a properly designed, tumor-targeted contrast agent may be useful to stage cancer and guide the surgical resection of only those nodes which are cancer positive. Moreover, non-invasive NIRF functional lymphatic imaging may provide diagnostics and information in lymphatic response to therapy as mechanism of therapeutic action, including surgery and emerging anti-lymphangiogenic treatments.[1,53]

Clinical Studies

Studies were conducted under the University of Texas Health Science Center at Houston and M.D. Anderson Cancer Center (MDACC) Institutional Review Boards and the Food and Drug Administration (FDA, IND #106,345) under protocol Lymphatic Imaging in Melanoma. Unfortunately we were unable to image the subjects prior to the initial tumor biopsy as the subjects present at MDACC only after the official diagnosis of melanoma is made by an outside primary care physician. To date, four of eighteen proposed subjects have been recruited. After informed consent and just prior to undergoing wide-local excision and SLN biopsy, each subject received two intradermal injections of 25 μg ICG diluted in 0.1 mL of saline (322 μM ICG) near but distal to the primary tumor biopsy site. Similar injections were administered at the corresponding locations on the contralateral limb to provide images of control lymphatics. NIRF images of the draining lymphatics on the diseased and control limbs were acquired for approximately 10 min. As part of a secondary longitudinal study of post-surgical lymphatic recovery, additional intradermal injections, total dose ≤400 μg ICG, were then administered in bilateral limbs and NIRF images of each limb were acquired for approximately 30 more min to establish a baseline of overall lymphatic structure and function. Each injection site was covered with a small band-aid and, if necessary to prevent oversaturation of the camera, black vinyl tape. The subject's vital signs were monitored for 2 h followed by a 24 h phone call to screen for signs of allergic reaction to the ICG. No adverse events have been reported in this study, although subjects in

other studies have developed erythema around the injection sites immediately after injection and were given a single dose of Benadryl to resolve any allergic reaction.

In two of the four subjects imaged to date, we observed no apparent reorganization of the draining lymphatics on the diseased limb as shown in Fig. 6. Interestingly in both cases, a fluorescent lymphatic vessel passed directly under the primary tumor biopsy site. In the other subjects, distinct architectural differences were observed in the draining lymphatics on the diseased limb as compared to the control limbs as shown in Fig. 7. As shown in Fig. 7b, the draining lymphatics on the diseased limb were more tortuous and numerous while the lymphatics on the contralateral limb appeared to be more linear with a single lymphatic vessel draining each injection site. In these two cases and including only those lymphatic vessels at least 3.5 cm long, the average tortuosity ratios were 1.27 ± 0.13 ($n = 9$) and 1.08 ± 0.04 ($n = 6$) for the diseased and contralateral limb lymphatics respectively. Using a standard t-test, the difference in the average tortuosity ratios was determined to be significant with a p-value of 0.006. Intraoperative images of the SLN were also acquired and as shown in Fig. 7d, the sentinel node was fluorescent and easily identified with NIRF imaging. In each case, the SLNs were tumor free and future studies need to be performed to see if lymphatic reorganization and/or contractile function relate to nodal status. Contractile lymphatic function was also observed in the diseased limbs of all four subjects. Although increased lymphatic flow has been implicated in animal models of metastatic melanoma, [16,39] additional studies are needed to determine the effect primary and metastatic tumors have on contractile function in humans as has been demonstrated in preclinical models.[23]

To our knowledge, these images represent the first non-invasive images of lymphatics in melanoma patients using *microdose amounts* of ICG, however, they only provide a snapshot in time of the lymphatics, and additional studies are required to elucidate how lymphatics change due to tumor growth over time and particularly in preparation for and during metastasis.

DISCUSSION AND SUMMARY

In this contribution we reviewed NIRF imaging and its use in preclinical and clinical applications including SNL mapping, intraoperative guidance, assessment of lymphatic architecture and function in health and disease, and efficacy assessment of lymphatic therapies. We also presented initial images from an ongoing clinical feasibility study which illustrate the ability to non-invasively and macroscopically image architectural changes in the draining lymphatics of a limb with melanoma, previously only seen through histopathologic studies. Although two of the four subjects recruited to date had networks of more tortuous lymphatics and all four had active lymphatic pumping, not one had metastatic disease in the sentinel nodes, and no correlation of lymphatic architecture or function with metastatic disease could be made at this early stage of the study. As such continued studies are needed to determine whether NIRF imaging can provide a clinically relevant, non-invasive means to assess tumor involvement in the lymphatics and a means to monitor lymphatic recovery following lymphatic trauma as a result of cancer treatment and to determine effectiveness of treatment.

Studies are also needed to determine whether the observed differences in the draining lymphatics on the diseased limb and the corresponding contralateral lymphatics are a result of cellular signaling by tumor-excreted lymphangiogenic factors such as VEGF-C,[17] mechanical obstruction due to the presence of the tumor, normal wound healing following the trauma associated with tumor biopsy, or some combination thereof. Unfortunately we were unable to image the subjects prior to biopsy as the subjects present at MDACC only

after the official diagnosis of melanoma was made by an outside primary care physician, and, as such, we are unable to completely rule out the effect the biopsy may have had on the lymphatics. While the exact causes of lymphatic reorganization are unknown, the lymphatic changes observed in the mouse model (Fig. 4) suggest that tumor growth itself could play a role in the lymphatic remodeling observed in the diseased limbs. It is also interesting to note that the primary tumor in both subjects with more tortuous lymphatics was located on the foot where networks of smaller, more superficial lymphatic vessels may more readily facilitate lymphatic reorganization than the larger, deeper lymphatic trunks found in the legs and upper arms.

While NIRF lymphatic imaging has shown versatility and potential as a clinical imaging modality, additional improvements in the technique are needed to facilitate full clinical translation and acceptance. The visualization of fine lymphatic structure and contractile propulsion of the lymphatics is governed by the sensitivity of the NIRF imaging system. Excitation light leakage is typically the largest single source of noise in fluorescence imaging due to the large quantities of backscattered excitation light. Special attention must be made during the selection and positioning of the optics and optical filters to ensure optimal rejection levels and increased sensitivity. The more sensitive the imaging system, the lower the quantity of contrast agent required for visualization of the lymphatics. The sensitivity of the instrument and quantity of contrast agent appear to play a critical role in the observation of propulsive lymph flow, as we are the only group to date that has reported visualizing contractile lymphatic pumping using NIRF imaging. We believe this is due to the sensitivity of our device[29] which enables us to use microdose amounts of fluorophore reducing the potential to over saturate the lymphatic vessels with fluorophore possibly masking the slight variations in dye concentration observed during lymphatic contraction and minimizing any negative effects the exogenous fluorophore may have on lymphatic contractile function. Standardized figures of merit are needed to compare NIRF instrumentation both for preclinical and clinical use.

Perhaps the most significant limitation of NIRF imaging in large tissue volumes is the attenuation of light due to photon scatter. While many lymphatics are superficial and easily observed using non-invasive NIRF imaging, as lymphatic vessels promulgate deeper into the tissue the increased scatter results in a broadening of its observed structure until, depending on the depth, its fluorescently stained vasculature becomes indistinguishable from background signal. As such, deep lymphatics such as those in the gastroin-testinal compartment and possibly in morbidly obese subjects may not be resolved non-invasively. Brighter dyes with higher quantum yields and more sensitive detection instrumentation will improve imaging depth, however, significant advances in the non-invasive resolution of deep lymphatics will likely depend on further development of brighter NIRF dyes and the frequency-domain photon migration instrumentation and algorithms which may lead to more robust and clinically relevant NIRF tomography.

In conclusion, NIRF imaging is a new imaging modality that can provide unprecedented images of the lymphatics *in vivo*, potentially opening the way for rapid, clinical assessment of lymphatic architecture and contractile function currently unavailable using the traditional medical imaging modalities. Because of the safety history of ICG, the low risk associated with microdose amounts of ICG and other contrast agents, and the small size and relatively low cost of the instrumentation, NIRF imaging may someday be readily available in the doctor’s office facilitating the “point-of-care” diagnosis of lymphatic disease and the assessment of lymphatic response to therapy. As NIRF imaging and additional contrast agents, which can be targeted for specific biological markers, become available, additional insights into the role of the lymphatics in cancer and other common diseases may be elucidated potentially opening new avenues for treatments not currently available.

Supplementary Material

Refer to Web version on PubMed Central for supplementary material.

Acknowledgments

The authors acknowledge I-Chih Tan and Banghe Zhu for their technical contributions and Melissa B. Aldrich, Kristen E. Adams, Chinmay Darne, Caroline E. Fife, Renie Guilliod, Milton V. Marshall, Erik A. Maus, Latisha A. Smith, I-Chih Tan, and Banghe Zhu for insightful discussions and participation in the clinical studies. This work was supported in parts by grants from the U.S. National Institutes of Health, National Cancer Institute (R01 CA 128919), the National Cancer Institute Network for Translational Research (U54 CA136404), and the National Heart, Lung, and Blood Institute (R01 HL092923).

ABBREVIATIONS

ICG	Indocyanine green
NIR	Near-infrared
NIRF	Near-infrared fluorescence
MRI	Magnetic resonance imaging
CCD	Charge coupled device
PET	Positron emission tomography
CT	X-ray computed tomography
p.i	Post implantation
LN	Lymph node
SLN	Sentinel lymph node
MLD	Manual lymphatic drainage
GD	Gadobenate dimeglumine
ROI	Region of interest
FBS	Fetal bovine serum
IND	Investigational new drug application
IRB	Institutional review board
FDA	Food and Drug Administration
ICCD	Intensified charge coupled device

References

1. Achen MG, Mann GB, Stacker SA. Targeting lymphangiogenesis to prevent tumour metastasis. Br J Cancer. 2006; 94(10):1355–1360. [PubMed: 16641900]
2. Adams KE, Ke S, Kwon S, Liang F, Fan Z, Lu Y, Hirschi K, Mawad ME, Barry MA, Sevick-Muraca EM. Comparison of visible and near-infrared wavelength- excitable fluorescent dyes for molecular imaging of cancer. J Biomed Opt. 2007; 12(2):024017. [PubMed: 17477732]
3. Adams KE, Rasmussen JC, Darne C, Tan IC, Aldrich MB, Marshall MV, Fife CE, Maus EA, Smith LA, Guilloid R, Hoy S, Sevick-Muraca EM. Direct evidence of improved lymphatic function following treatment with an advanced pneumatic compression device. Biomed Opt Express. 2010; 1(1):114–125. [PubMed: 21258451]
4. Barrett T, Choyke PL, Kobayashi H. Imaging of the lymphatic system: new horizons. Contrast Media Mol Imaging. 2006; 1(6):230–245. [PubMed: 17191764]

5. Corlu A, Choe R, Durduran T, Rosen MA, Schweiger M, Arridge SR, Schnall MD, Yodh AG. Three-dimensional in vivo fluorescence diffuse optical tomography of breast cancer in humans. Opt Express. 2007; 15(11):6696–6716. [PubMed: 19546980]
6. Cormier JN, Askew RL, Mungovan KS, Xing Y, Ross MI, Armer JM. Lymphedema beyond breast cancer. Cancer. 2010; 116(22):5138–5149. [PubMed: 20665892]
7. Dadras SS, Lange-Asschenfeldt B, Velasco P, Nguyen L, Vora A, Muzikansky A, Jahnke K, Hauschild A, Hirakawa S, Mihm MC, Detmar M. Tumor lymphangiogenesis predicts melanoma metastasis to sentinel lymph nodes. Mod Pathol. 2005; 18(9):1232–1242. [PubMed: 15803182]
8. Davies-Venn C, Angermiller B, Wilganowski N, Ghosh P, Harvey B, Wu G, Kwon S, Aldrich M, Sevick-Muraca E. Albumin-binding domain conjugate for near-infrared fluorescence lymphatic imaging. Mol Imaging Biol. 10.1007/s11307-011-0499-x
9. Eichholz A, Merchant S, Gaya AM. Anti-angiogenesis therapies: their potential in cancer management. OncoTargets Ther. 2010; 3(1):69–82.
10. Florey H. Observations on the contractility of lacteals: part I. J Physiol. 1927; 62(3):267–272. [PubMed: 16993848]
11. Folkman J. Tumor angiogenesis: therapeutic implications. N Engl J Med. 1971; 285(21):1182–1186. [PubMed: 4938153]
12. Fujiwara M, Mizukami T, Suzuki A, Fukamizu H. Sentinel lymph node detection in skin cancer patients using real-time fluorescence navigation with indocyanine green: preliminary experience. J Plast Reconstr Aesthet Surg. 2008; 62:e373–e378. [PubMed: 18556255]
13. Godavarty A, Sevick-Muraca EM, Eppstein MJ. Three-dimensional fluorescence lifetime tomography. Med Phys. 2005; 32(4):992–1000. [PubMed: 15895582]
14. Guidance for Industry. Investigators, and Reviewers: Exploratory IND Studies. U.S. Department of Health and Human Services, Food and Drug Administration CDER; Rockville, MD: 2006.
15. Hanahan D, Weinberg RA. The hallmarks of cancer. Cell. 2000; 100(1):57–70. [PubMed: 10647931]
16. Harrell MI, Iritani BM, Ruddell A. Tumor-induced sentinel lymph node lymphangiogenesis and increased lymph flow precede melanoma metastasis. Am J Pathol. 2007; 170(2):774–786. [PubMed: 17255343]
17. Hirakawa S, Brown LF, Kodama S, Paavonen K, Alitalo K, Detmar M. VEGF-C-induced lymphangiogenesis in sentinel lymph nodes promotes tumor metastasis to distant sites. Blood. 2007; 109(3):1010–1017. [PubMed: 17032920]
18. Houston JP, Ke S, Wang W, Li C, Sevick-Muraca EM. Quality analysis of in vivo near-infrared fluorescence and conventional gamma images acquired using a dual-labeled tumor-targeting probe. J Biomed Opt. 2005; 10(5):054010. [PubMed: 16292970]
19. Jain RK. Antiangiogenic therapy for cancer: current and emerging concepts. Anglais. 2005; 19(4 Suppl 3):7–16.
20. Joshi A, Bangerth W, Hwang K, Rasmussen JC, Sevick-Muraca EM. Fully adaptive FEM based fluorescence optical tomography from time-dependent measurements with area illumination and detection. Med Phys. 33(5):1299–1310.2006; [PubMed: 16752565]
21. Kitai T, Inomoto T, Miwa M, Shikayama T. Fluorescence navigation with indocyanine green for detecting sentinel lymph nodes in breast cancer. Breast Cancer. 2005; 12(3):211–215. [PubMed: 16110291]
22. Kwon S, Sevick-Muraca EM. Noninvasive quantitative imaging of lymph function in mice. Lymphat Res Biol. 2007; 5(4):219–231. [PubMed: 18370912]
23. Kwon S, Sevick-Muraca EM. Functional lymphatic imaging in tumor-bearing mice. J Immunol Methods. 2010; 360(1–2):167–172. [PubMed: 20600076]
24. Kwon S, Sevick-Muraca EM. Mouse phenotyping with near-infrared fluorescence lymphatic imaging. Biomed Opt Express. 2011; 2(6):1403–1411. [PubMed: 21698004]
25. Lee AC, Keshtgar MR, Waddington WA, Ell PJ. The role of dynamic imaging in sentinel lymph node biopsy in breast cancer. Eur J Cancer. 2002; 38(6):784–787. [PubMed: 11937312]
26. Liu NF, Lu Q, Jiang ZH, Wang CG, Zhou JG. Anatomic and functional evaluation of the lymphatics and lymph nodes in diagnosis of lymphatic circulation disorders with contrast magnetic resonance lymphangiography. J Vasc Surg. 2009; 49(4):980–987. [PubMed: 19223143]

27. Lucarelli RT, Ogawa M, Kosaka N, Turkbey B, Kobayashi H, Choyke PL. New approaches to lymphatic imaging. Lymphat Res Biol. 2009; 7(4):205–214. [PubMed: 20143919]
28. Marshall MV, Draney D, Sevick-Muraca EM, Olive DM. Single-dose intravenous toxicity study of IRDye 800CW in Sprague-Dawley rats. Mol Imaging Biol. 2010; 12(6):583–594. [PubMed: 20376568]
29. Marshall MV, Rasmussen JC, Tan IC, Aldrich MB, Adams KE, Wang X, Fife CE, Maus EA, Smith LA, Sevick-Muraca EM. Near-infrared fluorescence imaging in humans with indocyanine green: a review and update. Open Surg Oncol J. 2010; 2:12–25.
30. Maus EA, Tan IC, Rasmussen JC, Marshall MV, Fife CE, Smith LA, Guilliod R, Sevick-Muraca EM. Near-infrared fluorescence imaging of lymphatics in head and neck lymphedema. Head Neck. 10.1002/hed.21538
31. Miyashiro I, Miyoshi N, Hiratsuka M, Kishi K, Yamada T, Ohue M, Ohigashi H, Yano M, Ishikawa O, Imaoka S. Detection of sentinel node in gastric cancer surgery by indocyanine green fluorescence imaging: comparison with infrared imaging. Ann Surg Oncol. 2008; 15(6):1640–1643. [PubMed: 18379850]
32. Norrmen C, Tammela T, Petrova TV, Alitalo K. Biological basis of therapeutic lymphangiogenesis. Circulation. 2011; 123(12):1335–1351. [PubMed: 21444892]
33. Ntziachristos V, Yodh AG, Schnall M, Chance B. Concurrent MRI and diffuse optical tomography of breast after indocyanine green enhancement. Proc Natl Acad Sci USA. 2000; 97(6):2767–2772. [PubMed: 10706610]
34. Ogasawara Y, Ikeda H, Takahashi M, Kawasaki K, Doihara H. Evaluation of breast lymphatic pathways with indocyanine green fluorescence imaging in patients with breast cancer. World J Surg. 2008; 32(9):1924–1929. [PubMed: 18330628]
35. Ogata F, Azuma R, Kikuchi M, Koshima I, Morimoto Y. Novel lymphography using indocyanine green dye for near-infrared fluorescence labeling. Ann Plast Surg. 2007; 58(6):652–655. [PubMed: 17522489]
36. Ogata F, Narushima M, Mihara M, Azuma R, Morimoto Y, Koshima I. Intraoperative lymphography using indocyanine green dye for near-infrared fluorescence labeling in lymphedema. Ann Plast Surg. 2007; 59(2):180–184. [PubMed: 17667413]
37. Oremus, A.; Walker, K.; Dayes, I.; Raina, P. Diagnosis and treatment of secondary lymphedema. McMaster University Evidence-based Practice Center for Agency for Healthcare Research and Quality; Draft version; October 19. 2009
38. Polom K, Murawa D, Rho Y-s, Nowaczyk P, Hünerbein M, Murawa P. Current trends and emerging future of indocyanine green usage in surgery and oncology. Cancer. 2011; 117(21): 4812–4822. [PubMed: 21484779]
39. Proulx ST, Luciani P, Derzsi S, Rinderknecht M, Mumprecht V, Leroux JC, Detmar M. Quantitative imaging of lymphatic function with liposomal indocyanine green. Cancer Res. 2010; 70(18):7053–7062. [PubMed: 20823159]
40. Qian CN, Berghuis B, Tsarfaty G, Bruch M, Kort EJ, Ditlev J, Tsarfaty I, Hudson E, Jackson DG, Petillo D, Chen JD, Resau JH, Teh BT. Preparing the “soil”: the primary tumor induces vasculature reorganization in the sentinel lymph node before the arrival of metastatic cancer cells. Cancer Res. 2006; 66(21):10365–10376. [PubMed: 17062557]
41. Radhakrishnan K, Rockson SG. The clinical spectrum of lymphatic disease. Ann N Y Acad Sci. 2008; 1131(1):155–184. [PubMed: 18519969]
42. Ran S, Volk L, Hall K, Flister MJ. Lymphangiogenesis and lymphatic metastasis in breast cancer. Pathophysiology. 2010; 17(4):229–251. [PubMed: 20036110]
43. Rasmussen JC I, Tan C, Marshall MV, Adams KE, Kwon S, Fife CE, Maus EA, Smith L, Covington KR, Sevick-Muraca EM. Human lymphatic architecture and dynamic transport imaged using near-infrared fluorescence. Transl Oncol. 2010; 3(6):362–372. [PubMed: 21151475]
44. Rasmussen JC I, Tan C, Marshall MV, Fife CE, Sevick-Muraca EM. Lymphatic imaging in humans with near-infrared fluorescence. Curr Opin Biotechnol. 2009; 20(1):74–82. [PubMed: 19233639]
45. Rinderknecht M, Detmar M. Tumor lymphangiogenesis and melanoma metastasis. J Cell Physiol. 2008; 216(2):347–354. [PubMed: 18481261]

46. Schaafsma BE, Mieog JSD, Hutteman M, van der Vorst JR, Kuppen PJK, Löwik CWGM, Frangioni JV, van de Velde CJH, Vahrmeijer AL. The clinical use of indocyanine green as a near-infrared fluorescent contrast agent for image-guided oncologic surgery. J Surg Oncol. 2011; 104(3):323–332. [PubMed: 21495033]
47. Sevick-Muraca EM, Sharma R, Rasmussen JC, Marshall MV, Wendt JA, Pham HQ, Bonefas E, Houston JP, Sampath L, Adams KE, Blanchard DK, Fisher RE, Chiang SB, Elledge R, Mawad ME. Imaging of lymph flow in breast cancer patients after microdose administration of a near-infrared fluorophore: feasibility study. Radiology. 2008; 246(3):734–741. [PubMed: 18223125]
48. Sharma R, Wang W, Rasmussen JC, Joshi A, Houston JP, Adams KE, Cameron A, Ke S, Kwon S, Mawad ME, Sevick-Muraca EM. Quantitative imaging of lymph function. Am J Physiol Heart Circ Physiol. 2007; 292(6):H3109–H3118. [PubMed: 17307997]
49. Smith RO. Lymphatic contractility. J Exp Med. 1949; 90(5):497–509. [PubMed: 18143591]
50. Stacker SA, Achen MG, Jussila L, Baldwin ME, Alitalo K. Metastasis: lymphangiogenesis and cancer metastasis. Nat Rev Cancer. 2002; 2(8):573–583. [PubMed: 12154350]
51. Stuker F, Ripoll J, Rudin M. Fluorescence molecular tomography: principles and potential for pharmaceutical research. Pharmaceutics. 2011; 3(2):229–274.
52. Tagaya N, Yamazaki R, Nakagawa A, Abe A, Hamada K, Kubota K, Oyama T. Intraoperative identification of sentinel lymph nodes by near-infrared fluorescence imaging in patients with breast cancer. Am J Surg. 2008; 195(6):850–853. [PubMed: 18353274]
53. Tammela T, Saaristo A, Holopainen T, Yla-Herttuala S, Andersson LC, Virolainen S, Immonen I, Alitalo K. Photodynamic ablation of lymphatic vessels and intralymphatic cancer cells prevents metastasis. Sci Transl Med. 2011; 3(69):69ra11.
54. Tan IC, Maus EA, Rasmussen JC, Marshall MV, Adams KE, Fife CE, Smith LA, Chan W, Sevick-Muraca EM. Assessment of lymphatic contractile function after manual lymphatic drainage using near-infrared fluorescence imaging. Arch Phys Med Rehabil. 2011; 92(5):756–764.e1. [PubMed: 21530723]
55. Tanaka E, Choi HS, Fujii H, Bawendi MG, Frangioni JV. Image-guided oncologic surgery using invisible light: completed pre-clinical development for sentinel lymph node mapping. Ann Surg Oncol. 2006; 13(12):1671–1681. [PubMed: 17009138]
56. Thompson AB, Sevick-Muraca EM. Near-infrared fluorescence contrast-enhanced imaging with intensified charge-coupled device homodyne detection: measurement precision and accuracy. J Biomed Opt. 2003; 8(1):111–120. [PubMed: 12542387]
57. Unno N, Inuzuka K, Suzuki M, Yamamoto N, Sagara D, Nishiyama M, Konno H. Preliminary experience with a novel fluorescence lymphography using indocyanine green in patients with secondary lymphedema. J Vasc Surg. 2007; 45(5):1016–1021. [PubMed: 17391894]
58. Unno N, Nishiyama M, Suzuki M, Yamamoto N, Inuzuka K, Sagara D, Tanaka H, Konno H. Quantitative lymph imaging for assessment of lymph function using indocyanine green fluorescence lymphography. Eur J Vasc Endovasc Surg. 2008; 36(2):230–236. [PubMed: 18534875]
59. Yuan Z, Chen L, Luo Q, Zhu J, Lu H, Zhu R. The role of radionuclide lymphoscintigraphy in extremity lymphedema. Ann Nucl Med. 2006; 20(5):341–344. [PubMed: 16878705]
60. Zhang F, Niu G, Lu G, Chen X. Preclinical lymphatic imaging. Mol Imaging Biol. 2011; 13(4): 599–612. [PubMed: 20862613]
61. Zhou Q, Wood R, Schwarz EM, Wang YJ, Xing L. Near-infrared lymphatic imaging demonstrates the dynamics of lymph flow and lymphangiogenesis during the acute versus chronic phases of arthritis in mice. Arthritis Rheum. 2010; 62(7):1881–1889. [PubMed: 20309866]
62. Zhu B, Sevick-Muraca EM. Minimizing excitation light leakage and maximizing measurement sensitivity for molecular imaging with near-infrared fluorescence. J Innov Opt Health Sci. 2011; 4(3):301–307.
63. Zhu B, Tan I-C, Rasmussen JC, Sevick-Muraca EM. Validating the sensitivity and performance of near-infrared fluorescence imaging and tomography devices using a novel solid phantom and measurement approach. Technol Cancer Res Treat. (in press).

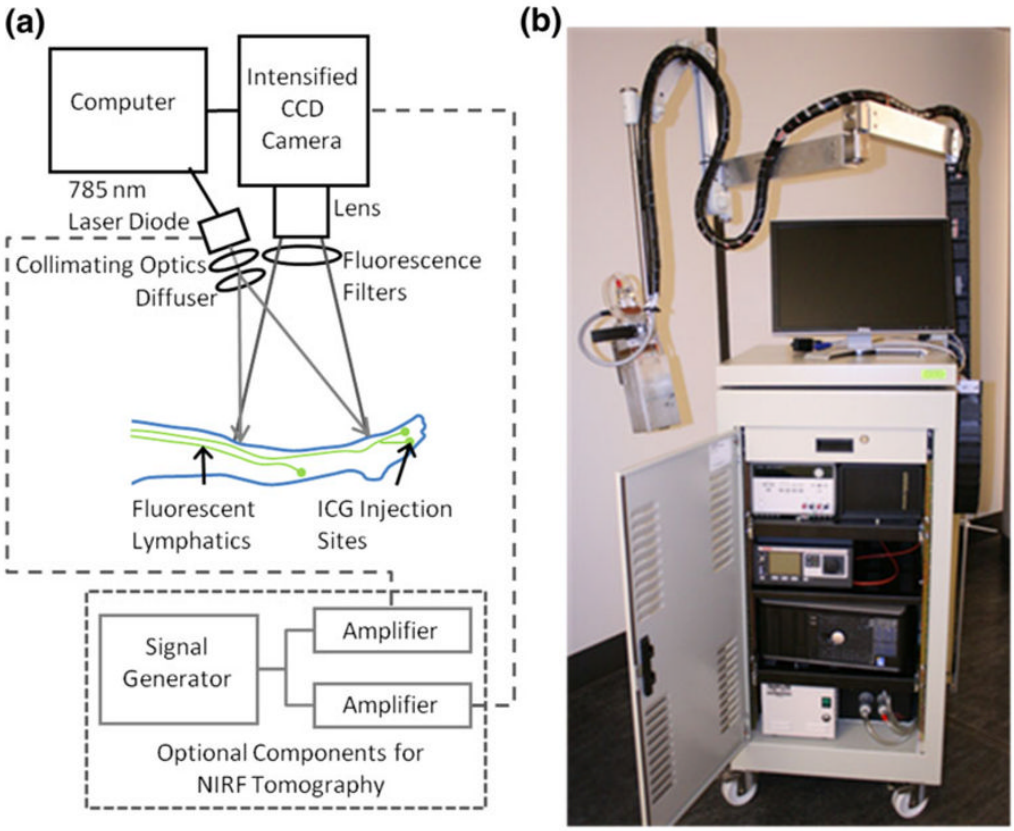

FIGURE 1.

(a) Schematic of a NIRF imaging system consisting of an excitation source, optical filters to selectively pass the NIR signal, and a CCD camera. Also shown are optional instrumentation which enable the acquisition of 'time-of-flight' information for NIRF tomography. (b) Image of a NIRF imaging system currently deployed for use in the operating room.

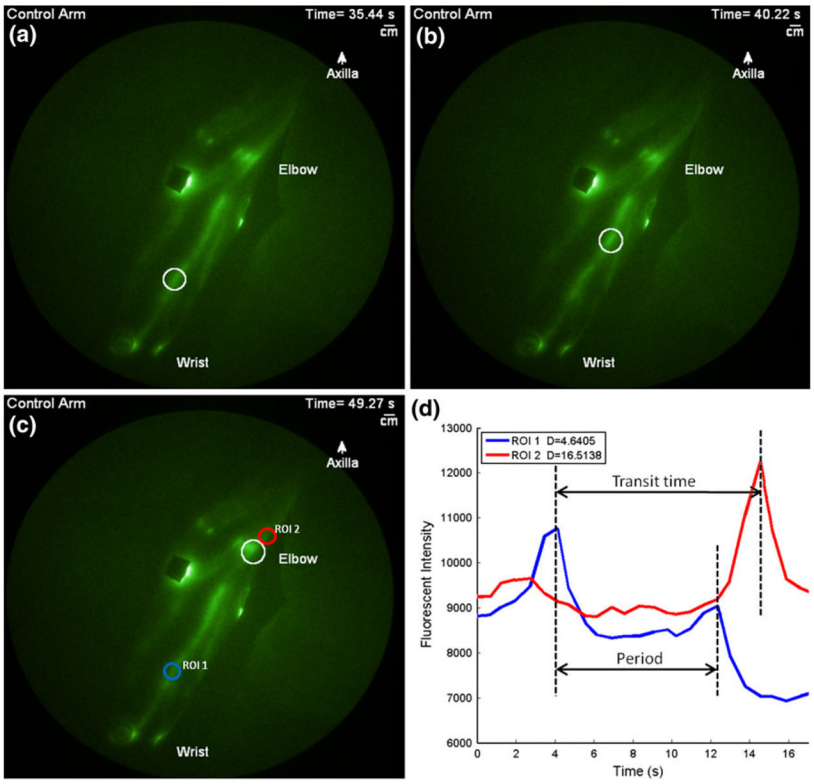

FIGURE 2.

(a–c) Series of images illustrating the propagation of bolus of fluorescent lymph (white circle) from the injection sites in a control arm towards the axillary nodal basin as shown in online Video 1. (d) Plot of the fluorescent intensity profiles for the ROIs in (c). Apparent lymph velocity is calculated as the ratio of the distance (D in the legend of (d)) between ROIs and the transit time. The period is the time lapse between consecutive propulsion events in the same ROI. Images are displayed in pseudo color.

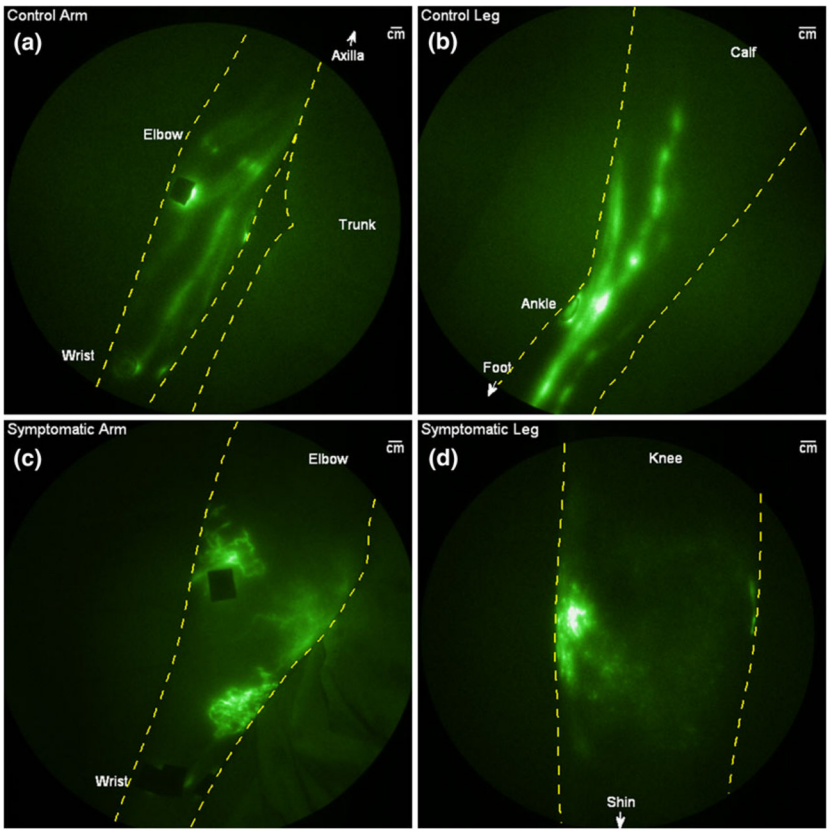

FIGURE 3.

Images of well-defined lymphatic vessels in the (a) arm of a healthy 38 year old female and (b) leg of a healthy 35 year old female and of abnormalities such as (c) tortuous vessels and diffuse networks of lymphatic capillaries seen in the arm of a 67 year old female with lymphedema and (d) diffuse or extravascular fluorescence in the leg of a 42 year old female with lymphedema. Images are displayed in pseudo color.

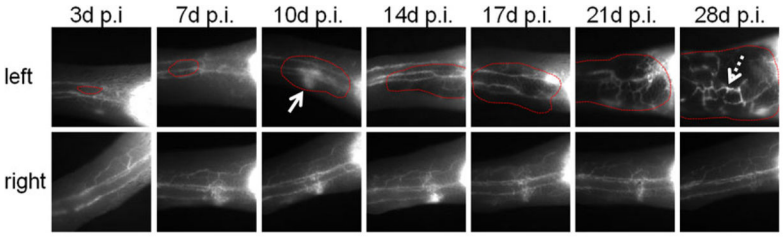

FIGURE 4.

Images illustrating the development of abnormal lymphatic drainage pathways and tortuous, dilated collecting lymphatic vessels in a mouse bearing melanoma (B16F10) in the dorsal aspect of the left foot (red) as compared to control right foot. Arrow indicates leakage of ICG and broken arrow tortuous and mispatterned lymphatic vessels.

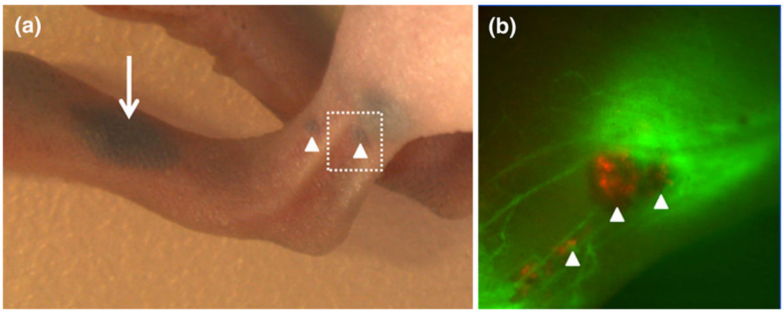

FIGURE 5.

(a) Image illustrating the primary melanoma (DsRed-B16F10) tumor (arrow) and in-transit metastases (arrowheads) in the left foot. (b) Fluorescent image of the lymphatics (green) and the in-transit metastases (red, arrowheads) near the lymphatic vessels.

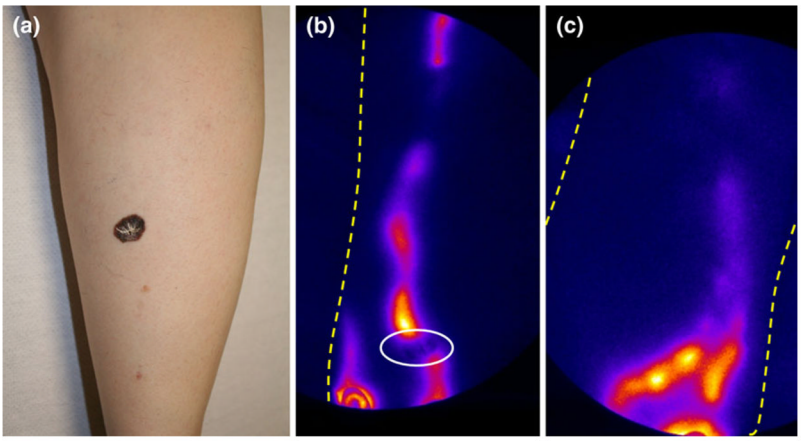

FIGURE 6.

(a) Color image of the tumor site (post biopsy) on the outer left foot of a 57 year old female with melanoma and NIRF images of the (b) healthy looking lymphatics near the melanoma site and (c) corresponding lymphatics on the contralateral limb. Circle is biopsy site, arrows show ICG injection sites. Images are displayed in pseudo color.

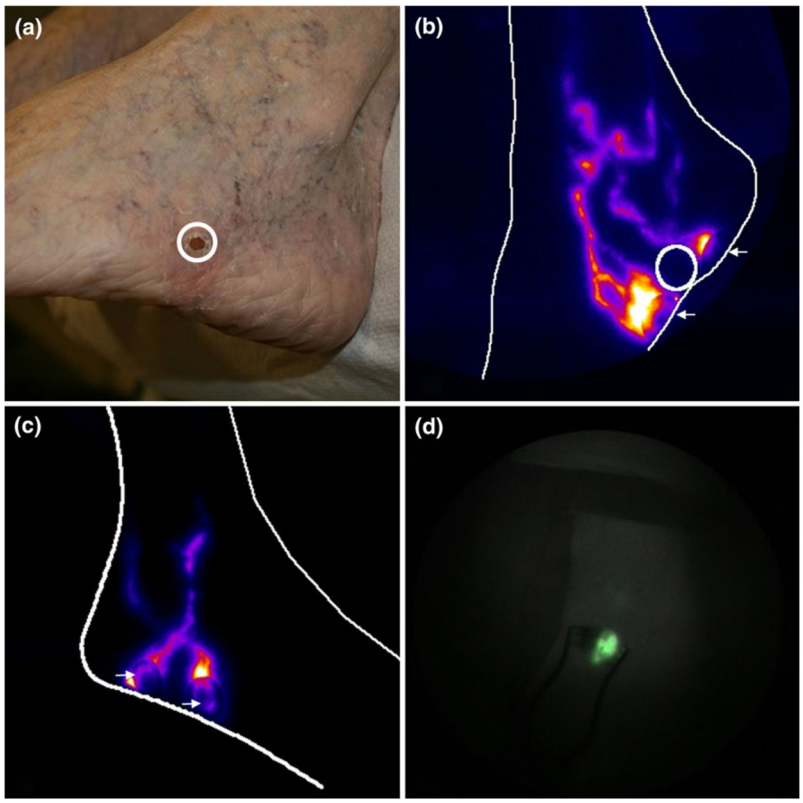

FIGURE 7.
(a) Color image of the tumor site (post biopsy) on the outer left foot of a 60 year old female with melanoma and NIRF images of (b) the tortuous lymphatics on the diseased foot, (c) the corresponding lymphatics on the contralateral limb, and (d) the SLN in the inguinal basin as seen during surgery. Circle is biopsy site, arrows show ICG injection sites. Images are displayed in pseudo color.